

# Optimal FOPI-FOPD controller design for rotary inverted pendulum system using grey wolves' optimization technique

Muhammad A. Hasan<sup>1</sup>, Ahmed A. Oglah<sup>1</sup>, Mehdi J. Marie<sup>2</sup>

<sup>1</sup>Control and Systems Engineering Department, Faculty of Engineering, University of Technology, Baghdad, Iraq

<sup>2</sup>Ministry of Industry and Minerals, Alzawraa Company, Baghdad, Iraq

## Article Info

### Article history:

Received Aug 11, 2022

Revised Oct 30, 2022

Accepted Nov 12, 2022

### Keywords:

Integer and fractional order PI-PD controllers

Optimization technique

RIP system

## ABSTRACT

The rotary inverted pendulum (RIP) has been used in various control application areas. This system can be represented as two degree of freedom (2-DOF), consisting of a rotating arm and rotating pendulum rod. RIP is an excellent example of designing a single-input multi-output (SIMO) system. Due to unstable RIP system dynamics, and its nonlinear model, multiple control techniques have been used to control this system. This paper uses integer and fractional order proportional integral-proportional derivative (PI-PD) controllers to stabilize the pendulum in the vertical direction. Constrained optimization approaches, such as the grey wolf optimization (GWO) methodology, are utilized to estimate the parametric values of the controllers. The simulation results showed that the fractional order PI-PD controller outperforms the integer order PI-PD controller with and without disturbance signal existence. A multiple results comparison has illustrated the superiority of fractional order controller over a previous work.

*This is an open access article under the [CC BY-SA](https://creativecommons.org/licenses/by-sa/4.0/) license.*



## Corresponding Author:

Muhammad A. Hassan

Control and Systems Engineering Department, Faculty of Engineering

University of Technology, Baghdad, Iraq

Email: cse.20.30@grad.uotechnology.edu.iq

## 1. INTRODUCTION

Rotary inverted pendulum (RIP) is a good example of control theory verification in control engineering. It is an excellent model for controlling space booster rocket attitude, satellite attitude control, autonomous plane landing systems, airplane stabilization in unsteady airflow, ship cabin stability, segway, and humanoid robots [1]. Also, this system has new applications, such as energy harvesting systems, which are considered an effective solution to excretion the kinetic energy from rotary systems where a pendulum system is connected to an electromagnetic generator [2]. Inverted pendulum systems are underactuated, unstable, nonlinear, open-loop, and challenging to handle. Due to its inherent nonlinearity, it is an interesting subject from a control standpoint. However, establishing an accurate mathematical model of the process using differential equations is typically difficult [3].

In the control engineering field, there are various types of inverted pendulums. Directional inverted pendulums [4], [5], double inverted pendulums [6], and RIP [7] are the most common. This study investigated the RIP type, which designed as a single-input multi-output (SIMO) system [8]. The stability of the RIP in the upright direction steadies the focus of most rotary inverted pendulum research. Various controllers have been utilized to regulate the RIP. We can summarize several researchers' work as: Sirisha and Junghare [9], used linear quadratic regulator (LQR), proportional integral derivative (PID), fuzzy logic, and  $H_\infty$  controllers to regulate the RIP performance and perform desirable stability. They did not assure the robustness of the controller, and the pendulum angle took a long time to settle. Ali and Naji in 2016 [10] suggested a state

feedback controller discipline the RIP behavior. The rod and arm angle response took a long time to reach the desired output with and without the parameter variation existence, considering the arm set point to be achieved at a very small magnitude (5 degrees). Sunil and Manju [11] have been introduced fuzzy logic controller to stabilize the RIP in the vertical direction. However, they did not check the system response after exerting an external impact, also, the arm response has not been listed. Lanjewar *et al.* [12] applied a fractional order PID controller to perform satisfied stability for the RIP system. The disturbance rejection was unacceptable when they applied 1.2 Nm as an external force. Öksüz *et al.* [13] proposed a full-state feedback controller for the system using MATLAB for a linear dynamic model. The results show that the system states response speed, but no robustness test is applied to the system.

The works listed above showd various control techniques utilized to stabilize RIP. The contribution of this work is summarizing the design of two closed-loop fractional-order proportional integral (PI) fractional order proportional derivative (PD) (FOPI-FOPD) control systems to control the RIP at the same time as a SIMO design approach, which is considered as one of the complex control systems. Rather than the complexity of this design, an optimization technique is accomplished to find the appropriate control system parameters. The modelling of RIP can be presented in this work using state-space representation, FOPI-FOPD, and integer PI-PD controllers that can be tuned by grey wolf optimization (GWO) technique used to control the RIP. The fractional order controllers (FOC) with appropriate performance outperform integer order controllers [14], [15]. The FOC like FOPD, FOPI, fractional order proportional integral derivative (FOPID), and FOPI-FOPD might perform better than integer-order [16], [17]. The quanser RIP is used in this work, as shown in Figure 1. An angle of  $\alpha$  displaces the pendulum. However,  $\theta$  is the rotating angle of the arm around the vertical axis.

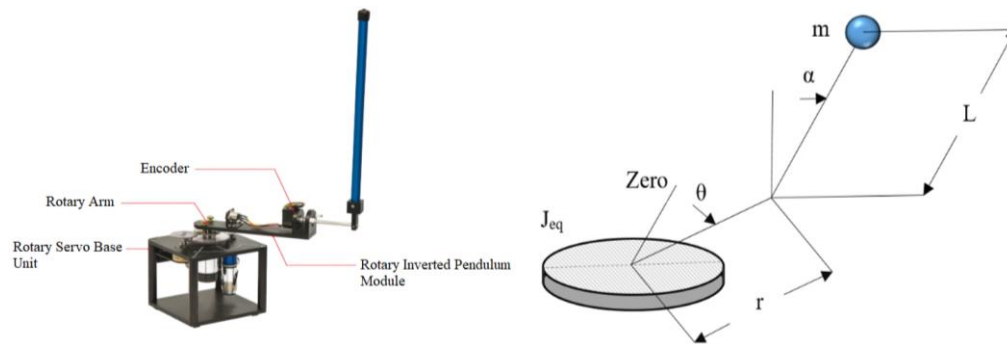


Figure 1. SRV-2 RIP model

## 2. MATHEMATICAL MODEL OF RIP

The rotating position of the RIP arm is obtained in Figure 1. The rod can be described as a lumped mass at mid length of the rod. The rod is moved by  $\alpha$  angle. However, the  $\theta$  depicts arm displacement at the  $x$ -axis. Therefore, a mathematical model can be created by inspection at the rotational velocity of the pendulum rod center of mass (COM). The terms used in system model derivations are listed in Table 1 [18].

Table 1. RIP system parameters

Variable	Description
$L$	Rod to COM displacement (m)
$m$	Arm mass (Kg)
$r$	Arm length (m)
$\theta$	Arm angle (radians)
$\alpha$	Rod deviation (radians)
$h$	Rod COM from the ground distance (m)
$J_{cm}$	Rod inertia about its COM (Kg.m <sup>2</sup> )
$V_x$	Rod velocity COM at the $x$ -direction (m/s)
$V_y$	Rod velocity COM at the $y$ -direction (m/s)

The velocity of the rod and arm can be expressed (1).

$$V_{(pendulum.center\ of\ mass)} = -L \cos \alpha (\dot{\alpha}) \hat{x} - L \sin \alpha (\dot{\alpha}) \hat{y} \quad (1)$$

$$V_{arm} = r \dot{\theta} \quad (2)$$

The (1) and (2) can be solved, so axes velocity is utilized (3).

$$V_x = r\dot{\theta} - L\cos\alpha (\dot{\alpha}) \quad (3)$$

$$V_y = -L\sin\alpha (\dot{\alpha}) \quad (4)$$

The Euler-Lagrange formulation has been used to obtain the system dynamic equations such as:

1) Potential energy: the system gravity energy is presented (5).

$$V = P.E(\text{pendulum}) = mgh = mgh L\cos\alpha \quad (5)$$

2) Kinetic energy: RIP system kinetic energies present (6).

$$T = K.E_{hub} + K.E_{vx} + K.E_{vy} + K.E_{pendulum} \quad (6)$$

The RIP rod's moment of inertia about its COM was presented subsequently as:

$$J_{cm} = \left(\frac{1}{12}\right)MR^2 \quad (7)$$

$$J_{cm} = \left(\frac{1}{12}\right)MR^2 = \left(\frac{1}{12}\right)M(2L^2) = \left(\frac{1}{3}\right)ML^2 \quad (8)$$

After substituting the (3), (4), (7), and (8) in (6), so system kinetic can be obtained (9).

$$T = \left(\frac{1}{2}\right)J_{eq} \dot{\theta}^2 + \left(\frac{1}{2}\right)m(r\dot{\theta} - L\cos\alpha (\dot{\alpha}))^2 + \left(\frac{1}{2}\right)m(-L\sin\alpha (\dot{\alpha}))^2 + \left(\frac{1}{2}\right)J_{cm} \dot{\alpha}^2 \quad (9)$$

The final Euler-Lagrange formulation can be expressed (10).

$$L = T - V = \left(\frac{1}{2}\right)J_{eq} \dot{\theta}^2 + \left(\frac{2}{3}\right)mL^2\dot{\alpha}^2 - mLr \cos\alpha (\dot{\alpha})(\dot{\theta}) + mr^2\dot{\theta}^2 - mgL\cos\alpha \quad (10)$$

When  $\theta$  and  $\alpha$  are the generalized coordinates, so:

$$\frac{\delta}{\delta t} \left( \frac{\delta L}{\delta \dot{\theta}} \right) - \frac{\delta L}{\delta \theta} = T_{output} - B_{eq} \dot{\theta} \quad (11)$$

$$\frac{\delta}{\delta t} \left( \frac{\delta L}{\delta \dot{\alpha}} \right) - \frac{\delta L}{\delta \alpha} = 0 \quad (12)$$

After linearizing the initial conditions, equations are modified as:

$$(J_{eq} + mr^2)\ddot{\theta} - mLr\ddot{\theta} = T_{output} - B_{eq}\dot{\theta} \quad (13)$$

$$\frac{4}{3}mL^2\ddot{\alpha} - mLr\ddot{\theta} - mgL\alpha = 0 \quad (14)$$

Then, the motor torque becomes:

$$T_{output} = \frac{\eta_m \eta_g K_t K_g (V_m - K_g K_m \dot{\theta})}{R_m} \quad (15)$$

RIP system state space can be illustrated (16).

$$\begin{bmatrix} \dot{\theta} \\ \dot{\alpha} \\ \ddot{\theta} \\ \ddot{\alpha} \end{bmatrix} = \begin{bmatrix} 0 & 0 & 1 & 0 \\ 0 & 0 & 0 & 1 \\ 0 & \frac{bd}{E} & \frac{-cG}{E} & 0 \\ 0 & \frac{qd}{E} & \frac{-bG}{E} & 0 \end{bmatrix} \begin{bmatrix} \theta \\ \alpha \\ \dot{\theta} \\ \dot{\alpha} \end{bmatrix} + \begin{bmatrix} 0 \\ 0 \\ c \frac{\eta_m \eta_g K_t K_g}{R_m E} \\ b \frac{\eta_m \eta_g K_t K_g}{R_m E} \end{bmatrix} V_m \quad (16)$$

Here,  $a = J_{eq} + mr^2$ ,  $b = mLr$ ,  $c = 4/3 mL^2$ ,  $d = mgL$ ,  $E = ac - b^2$  and  $G = \frac{\eta_m \eta_g K_t K_m K_g^2}{R_m}$ . The system specification can be listed as shown in Table 2.

Table 2. Typical SRV02 system specification

Symbol	Description	Value
$K_t$	Motor torque constant (N.m/A)	0.00767
$K_m$	Back EMF constant (V.s/radian)	00767
$R_m$	Armature resistance ( $\Omega$ )	2.6
$K_g$	SRV02 system gear ratio (motor $\rightarrow$ load)	14 (14 $\times$ 1)
$\eta_m$	Motor efficiency	0.69
$\eta_g$	Gearbox efficiency	0.9
$B_{eq}$	The equivalent viscous damping coefficient (N.m.s/radian)	1.5 e-3
$J_{eq}$	Equivalent moment of inertia at the load (Kg.m <sup>2</sup> )	9.31 e-4

After substituting the SRV02 system parameters values, then the system state space can be illustrated as:

$$\begin{bmatrix} \dot{\theta} \\ \dot{\alpha} \\ \dot{\theta} \\ \dot{\alpha} \end{bmatrix} = \begin{bmatrix} 0 & 0 & 1 & 0 \\ 0 & 0 & 0 & 1 \\ 0 & 39.32 & -14.52 & 0 \\ 0 & 81.78 & -13.98 & 0 \end{bmatrix} \begin{bmatrix} \theta \\ \alpha \\ \dot{\theta} \\ \dot{\alpha} \end{bmatrix} + \begin{bmatrix} 0 \\ 0 \\ 25.54 \\ 24.59 \end{bmatrix} V_m \quad (17)$$

$$Y = \begin{bmatrix} 1 & 0 & 0 & 0 \\ 0 & 1 & 0 & 0 \end{bmatrix} \begin{bmatrix} \theta \\ \alpha \end{bmatrix} + \begin{bmatrix} 0 \\ 0 \end{bmatrix} V_m \quad (18)$$

### 3. CONTROL SYSTEM SCHEME

#### 3.1. PI-PD and FOPI-FOPD controllers design

While the typical PID controller has limits in regulating such systems, the PI-PD controller structure offers an outstanding four-parameter controller for handling integrated, unsteady, and resonant systems to steady state adjustment [19]. PI-PD controller is a mathematical model-initiated theory. High-quality fulfillment can be gained at unstable and integrating processes [20], [21]. Figure 2 illustrates the PI-PD controller structure as PI and PD parts. Placing the system poles in required places can be achieved by interior feedback controller PD, on the other hand, the exterior loop is responsible for controlling the system after the interior loop action [22]. So, the PI-PD controller design has features of the traditional PID controller. In Figure 2,  $G_p(s)$  and  $D(s)$  present the controlled system and disturbance [23]. When  $G_p(s)$  is:

$$G_p(s) = \frac{N_p(s)}{D_p(s)} \quad (19)$$

PD and PI can be expressed as  $C_{FD}(s)$  and  $C_{PI}(s)$ , sequentially:

$$C_{FD}(s) = K_f + K_d(s) \quad (20)$$

$$C_{PI}(s) = K_p + \frac{K_i}{s} = \frac{K_p s + K_i}{s} \quad (21)$$

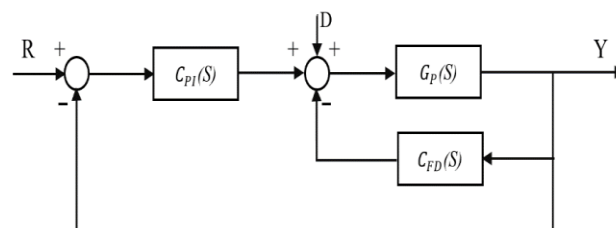


Figure 2. Single input single output control system with PI-PD controller [24]

Where  $N_p(s)$  is the numerator and  $D_p(s)$  is the denominator polynomials of the system transfer function,  $K_i$  is the integer gain,  $K_p$  is the feedforward gain,  $K_d$  is the derivative gain, and  $K_f$  is the proportional feedback gain. The approach design for FOPI-FOPD controller is the same as the integer PI-PD one, except the containing fractional integral and fractional derivative components. In addition to  $K_p$ ,  $K_i$ ,  $K_f$ , and  $K_d$ ,  $\mu$  order of differentiator,  $\lambda$  order of integrator represents the additional factors, which maximize the controller degree of flexibility to improve performance and achieve more robustness for the controlled system [25], [26]. The (22) and (23) illustrate the FOPI and FOPD mathematical description [27].

$$C_{FD}(S) = K_f + K_d S^\mu \tag{22}$$

$$C_{PI}(S) = K_p + \frac{K_i}{S^\lambda} \tag{23}$$

A PI-PD controller can be conducted by choosing  $\lambda = 1, \mu = 1$  [28]. Optimal performance can be achieved by fine-tuning the controller’s parameters. GWO technique has been used in this work to acquire the best minimizing error rate and reaching excellent stability by requiring the suitable controller parameter [16]. The integral time square error (ITSE) performance criteria have been applied as a cost function (24).

$$ITSE = \int_0^\infty te(t)^2 dt \tag{24}$$

The two loops of FOPI-FOPD and PI-PD controllers are designed to stabilize the RIP system in a SIMO design method illustrated in Figure 3 [29]. So the upright pendulum position and arm angle stabilization can simultaneously be achieved [30]. The SIMO structure of the RIP system requires the designing of two various controllers [31]. The first controller controls the arm, while the second controls the pendulum [32].

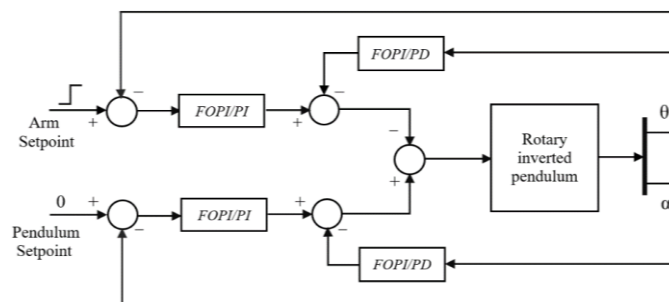


Figure 3. RIP SIMO controlled system illustration

**3.2. Optimization technique**

As control systems cannot accurately predict plant structure in the control system due to parameter uncertainty and uncertainty in plant models, soft computing based evolutionary algorithms can be used [33]. This work exploits the GWO technique to reduce the ITSE and acquire the best values of FOPI-FOPD and PI-PD controller’s factors [34], [35]. GWO is a conceptual program miming the grey wolf hunting strategy and social hierarchy. In nature, grey wolves live in a pack and have a stringent social hierarchy. On average, 5-12 participants in the group [36], [37]. Of specific weal is that they have a very rigorous social dominant hierarchy, as shown in Figure 4. The hierarchical social structure consists of four levels of gray wolves. The leader, alpha ( $\alpha$ ), is at the top of the pyramid. The alpha makes most choices about hunting. Followed by beta ( $\beta$ ), which supports the alpha in making decisions and carrying out other pack duties. The delta ( $\delta$ ) wolves provide the information about the wolves’ pack to alpha and beta. Omega ( $\omega$ ) is at the bottom of the pyramid, which always has to succumb to the other wolves [38], [39].

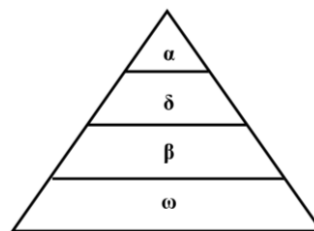


Figure 4. Grey wolf hierarchy

Grey wolves hunting can be presented as a theoretical equation. The alpha, beta, and delta have more knowledge than others about geography. So, we preserve the top three possibilities we have found so far and force the remaining search factors to update their placings in consideration of the best search factor’s position [40], which can be shown:

$$\vec{D}_\alpha = |\vec{C}_1 \cdot \vec{X}_\alpha - \vec{X}|, \vec{D}_\beta = |\vec{C}_2 \cdot \vec{X}_\beta - \vec{X}|, \vec{D}_\delta = |\vec{C}_3 \cdot \vec{X}_\delta - \vec{X}| \tag{25}$$

$$\vec{X}_1 = \vec{X}_\alpha - \vec{A}_1 \cdot (\vec{D}_\alpha), \vec{X}_2 = \vec{X}_\beta - \vec{A}_2 \cdot (\vec{D}_\beta), \vec{X}_3 = \vec{X}_\delta - \vec{A}_3 \cdot (\vec{D}_\delta) \tag{26}$$

$$\vec{X}(t + 1) = \frac{\vec{X}_1 + \vec{X}_2 + \vec{X}_3}{3} \tag{27}$$

Where  $\vec{X}_1, \vec{X}_2, \vec{X}_3$  are the best solution of  $(\alpha), (\beta),$  and  $(\delta),$  respectively.  $\vec{A}_1, \vec{A}_2, \vec{A}_3, \vec{C}_1, \vec{C}_2,$  and  $\vec{C}_3$  are the coefficient vectors, respectively, which can be presented as  $(\vec{A} = 2\vec{a} \cdot r_1$  and  $\vec{C} = 2 \cdot r_2)$ . Where,  $r_1$  and  $r_2$  is a random numbers between (0-1) and  $\vec{a}$  defined as linearly decreasing coefficient is changed from (0–2) [41].

#### 4. RESULTS AND DISCUSSION

The fractional and integer controllers have been applied to the RIP system to control the pendulum rod in the vertical position. The Simulink block diagram of the controlled system in Figure 5 shows the design of the controllers under the SIMO approach and a comparison between their results. Figure 6(a) illustrates the pendulum response and Figure 6(b) shows the unit step response of the arm for both controllers. Figure 6(c) illustrates the control signal behavior for both controllers. To achieve a fair comparison, the same parameters are used for both controllers with additional parameters of the fractional controller ( $\lambda$  and  $\mu$ ), which improve the system performance. It is obvious that the performance of the FOPI-FOPD controller is better than the PI-PD controller.

From Figure 6, the arm enters the state of equilibrium in less than one second without an overshoot for the FOPI-FOPD controller, while the PI-PD controller takes about two seconds to achieve the set point with a 13% overshoot. So, the pendulum rod entered the balancing state when the FOPI-FOPD controller was applied faster than it entered the equilibrium state when the PI-PD controller was applied. Although the swinging up of FOPI-FOPD is more than PI-PD, it did not exceed 0.04 rad. Figure 7(a) and Figure 7(b) illustrate the controller’s response behavior to the disturbance. As a result, the FOPI-FOPD controller was more robust than the PI-PD controller in the disturbance test.

The results of using the FOPI-FOPD and PI-PD controllers for RIP were illustrated in the preceding paragraphs. According to these findings, the time response characteristics acquired by the FOPI-FOPD controller are more suitable than those achieved by the PI-PD controller. The controller’s outputs are listed in Table 3. It indicates that the FOPI-FOPD controller can acquire a low control effort in addition to achieving desirable time response parameters, in terms of rise time ( $tr$ ), settling time ( $ts$ ), and overshoot ratio ( $Mp$ ).

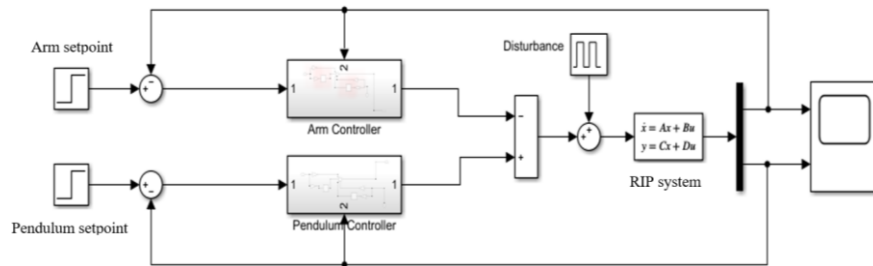


Figure 5. Simulink block diagram of the system controllers

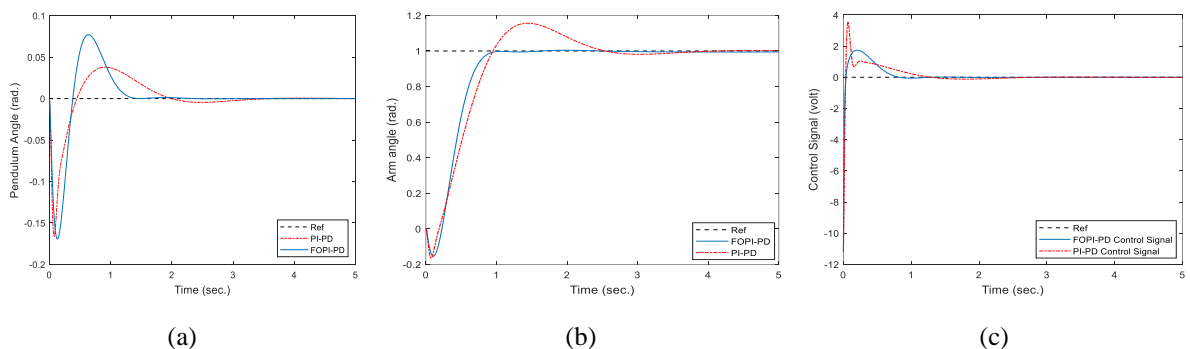


Figure 6. Simulation results of the balance control with the FOPI-FOPD and PI-PD: (a) pendulum response, (b) arm response, and (c) control signal behavior

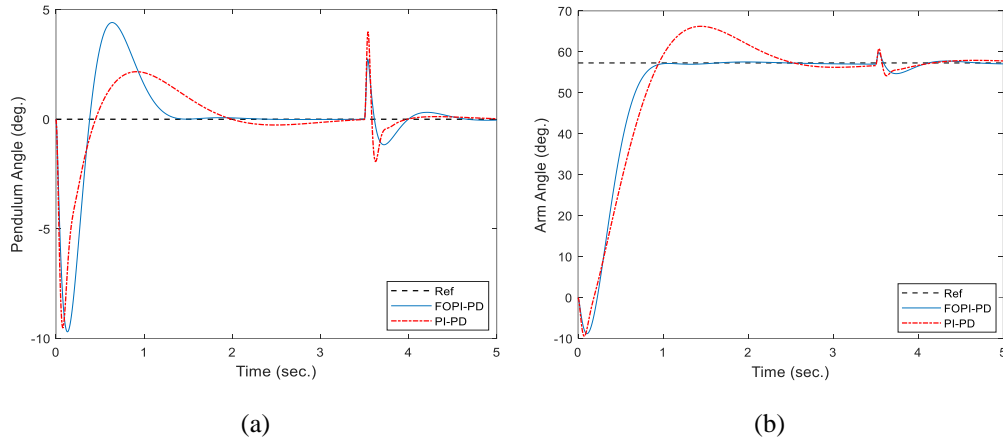


Figure 7. Simulation result after applying disturbance: (a) pendulum response and (b) arm response

Table 3. Controller’s performances comparison

Controller	Arm			Pendulum		
	<i>tr</i> (sec.)	<i>ts</i> (sec.)	<i>Mp</i> (%)	<i>tr</i> (sec.)	<i>ts</i> (sec.)	<i>Mp</i> (%)
FOPI-FOPD	0.422	0.781	–	0.172	1.174	46
PI-PD	0.591	2.153	13	0.271	1.710	23

A comparison of the proposed FOPI-FOPD controller’s performance with the performances of controllers created in earlier works (Table 4 and Table 5) shows its efficacy. It indicates that the FOPI-FOPD controller achieves the best transient response characteristics among previously studied controllers. The first comparison with model-free backstepping (MFBS) controller [42]. The same initial condition is considered for the FOPI-FOPD controlled system, as shown in Figure 8(a) and Figure 8(b).

A second comparison was presented with full-state (FSF) controller [13]. The same set point of the arm is taken and applied to the FOPI-FOPD controlled system, as shown in Figure 9(a) and Figure 9(b). The results proved that the proposed controller is more efficient than the FSF controller.

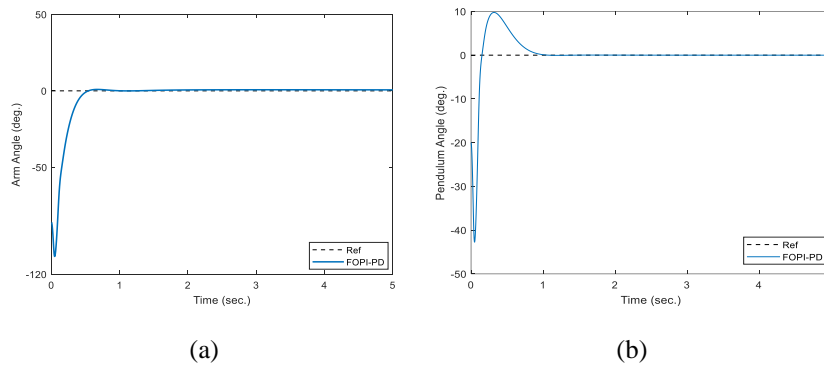


Figure 8. Simulation result after applying the same initial condition of search [42]: (a) arm response and (b) pendulum response

Table 4. Stabilization performance with previous work comparison

Controller	Arm			Pendulum		
	<i>tr</i> (sec.)	<i>ts</i> (sec.)	<i>Mp</i> (%)	<i>tr</i> (sec.)	<i>ts</i> (sec.)	<i>Mp</i> (%)
FOPI-FOPD	0.266	0.403	–	0.059	0.713	23
MFBS [42]	0.291	0.513	1	0.161	0.824	23

Table 5. Proposed controller versus previous work tracking performance comparison

Controller	Arm			Pendulum	
	<i>tr</i> (sec.)	<i>ts</i> (sec.)	<i>Mp</i> (%)	<i>tr</i> (sec.)	<i>Deviation</i> (degree)
FOPI-FOPD	0.442	0.781	–	0.172	-1.7 – 0.75
FSF [13]	0.925	1.107	–	0.181	-2 – 0.82

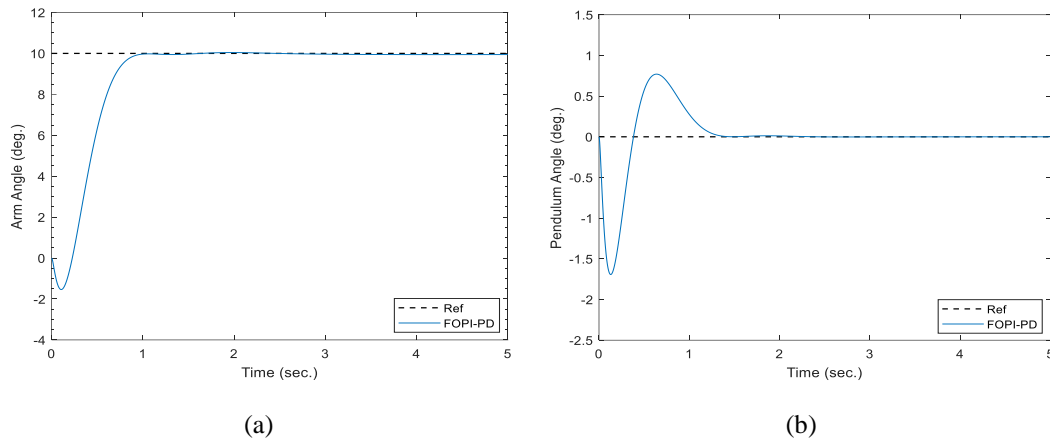


Figure 9. simulation result after applying the same setpoint of arms set of search [13]: (a) arm response and (b) pendulum response

## 5. CONCLUSION

The SIMO designs of FOPI-FOPD and PI-PD controllers for the RIP system are given in this paper. The GWO approach was used to determine the optimal parameters for both controller gains. The time response requirements and ITSE restrictions were incorporated into the suggested cost function to satisfy the needs of robustness and time response characteristics. The FOPI-FOPD was designed to improve system tracking. The suggested robust FOPI-FOPD controller was proved capable of driving the system, and the GWO approach was used to make the controller computationally efficient. Furthermore, the time response parameters achieved by the FOPI-FOPD controller are preferable to those acquired by the PI-PD controller and controllers developed previously.




## REFERENCES

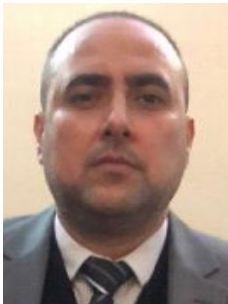
- [1] I. Chawla and A. Singla, "Real-Time Stabilization Control of a Rotary Inverted Pendulum Using LQR-Based Sliding Mode Controller," *Arabian Journal for Science and Engineering*, vol. 46, pp. 2589–2596, 2021, doi: 10.1007/s13369-020-05161-7.
- [2] E. Zaouali, F. Najjar, N. Kacem, and E. Foltete, "Pendulum-based embedded energy harvester for rotating systems," *Mechanical Systems and Signal Processing*, vol. 180, 2022, doi: 10.1016/j.ymssp.2022.109415.
- [3] X. Yang and X. Zheng, "Swing-Up and Stabilization Control Design for an Underactuated Rotary Inverted Pendulum System: Theory and Experiments," in *IEEE Transactions on Industrial Electronics*, vol. 65, no. 9, pp. 7229–7238, 2018, doi: 10.1109/TIE.2018.2793214.
- [4] K. J. Åström and K. Furuta, "Swinging up a pendulum by energy control," *Automatica*, vol. 36, no. 2, pp. 287–295, 2000, doi: 10.1016/S0005-1098(99)00140-5.
- [5] K. Yoshida, "Swing-up control of an inverted pendulum by energy-based methods," *Proceedings of the 1999 American Control Conference (Cat. No. 99CH36251)*, 1999, vol. 6, pp. 4045–4047, doi: 10.1109/ACC.1999.786297.
- [6] K. Furuta, T. Okutani, and H. Sone, "Computer control of a double inverted pendulum," *Computers & Electrical Engineering*, vol. 5, no. 1, pp. 67–84, 1978, doi: 10.1016/0045-7906(78)90018-6.
- [7] *Rotary Pendulum Workbook*, Markham, Ontario, Canada: Quanser Inc., 2011. [Online]. Available: [https://nps.edu/documents/105873337/0/Rotary+Pendulum+Workbook+\\_Instructor\\_.pdf/e17aa0a2-5f98-4957-b4a7-e80f0f52a4a3](https://nps.edu/documents/105873337/0/Rotary+Pendulum+Workbook+_Instructor_.pdf/e17aa0a2-5f98-4957-b4a7-e80f0f52a4a3)
- [8] D. H. Vu, S. Huang, and T. D. Tran, "Hierarchical robust fuzzy sliding mode control for a class of simo under-actuated systems with mismatched uncertainties," *TELKOMNIKA Telecommunication, Computing, Electronics and Control*, vol. 17, no. 6, 2019, doi: 10.12928/TELKOMNIKA.v17i6.13176.
- [9] V. Sirisha and A. S. Junghare, "A Comparative study of controllers for stabilizing a Rotary Inverted Pendulum," *International Journal of Chaos, Control, Modelling and Simulation (IJCCMS)*, vol. 3, no. 1/2, pp. 1–13, 2014, doi: 10.5121/ijccms.2014.3201.
- [10] H. I. Ali and R. M. Naji, "Optimal and Robust Tuning of State Feedback Controller for Rotary Inverted Pendulum," *Engineering and Technology Journal*, vol. 34, no. 15, pp. 2924–2939, 2016, doi: 10.30684/etj.34.15A.13.
- [11] A. Sunil and Manju G., "Quanser Rotary Inverted Pendulum Stabilization with Fuzzy Logic Controller," *International Research Journal of Engineering and Technology (IRJET)*, vol. 3, no. 6, pp. 2879–2882, 2016. [Online]. Available: <https://www.irjet.net/archives/V3/i6/IRJET-V3I6537.pdf>
- [12] A. Lanjewar, S. W. Khubalkar and A. S. Junghare, "Comparative Analysis of Two Loop Integer and Fractional Order PID Controller for Inverted Pendulum," *2018 International Conference on Smart Electric Drives and Power System (ICSEDPS)*, 2018, pp. 380–383, doi: 10.1109/ICSEDPS.2018.8536022.
- [13] M. Öksüz, M. B. Önal, R. Halicioğlu, and L. C. Dülger, "Alternative Controller Design for Rotary Inverted Pendulum," *Tehnički glasnik*, vol. 12, no. 3, pp. 139–145, 2018, doi: 10.31803/tg-20180208152214.
- [14] S. Y. Yousif and M. J. Mohamed, "Design of Robust FOPI-FOPD Controller for Maglev System Using Particle Swarm Optimization," *Engineering and Technology Journal*, vol. 39, no. 4A, pp. 653–667, 2021, doi: 10.30684/etj.v39i4a.1956.
- [15] G. A. R. Ibraheem, A. T. Azar, I. K. Ibraheem, and A. J. Humaidi, "A Novel Design of a Neural Network-Based Fractional PID Controller for Mobile Robots Using Hybridized Fruit Fly and Particle Swarm Optimization," *Complexity*, vol. 2020, 2020, doi: 10.1155/2020/3067024.
- [16] B. K. Dakua and B. B. Pati, "PIλ-PDμController for Suppression of Limit Cycle in Fractional-Order Time Delay System with






- Nonlinearities,” *2021 1st Odisha International Conference on Electrical Power Engineering, Communication and Computing Technology (ODICON)*, 2021, pp. 1-6, doi: 10.1109/ODICON50556.2021.9428971.
- [17] S. -W. Seo and H. H. Choi, “Digital Implementation of Fractional Order PID-Type Controller for Boost DC–DC Converter,” in *IEEE Access*, vol. 7, pp. 142652–142662, 2019, doi: 10.1109/ACCESS.2019.2945065.
- [18] M. Akhtaruzzaman and A. A. Shafie, “Modeling and control of a rotary inverted pendulum using various methods, comparative assessment and result analysis,” *2010 IEEE International Conference on Mechatronics and Automation*, 2010, pp. 1342–1347, doi: 10.1109/ICMA.2010.5589450.
- [19] N. Tan, “Computation of stabilizing PI-PD controllers,” *International Journal of Control, Automation and Systems*, vol. 7, pp. 175–184, 2009, doi: 10.1007/s12555-009-0203-y.
- [20] I. Kaya, “A PI-PD controller design for control of unstable and integrating processes,” *ISA Transactions*, vol. 42, no. 1, pp. 111–121, 2003, doi: 10.1016/s0019-0578(07)60118-9.
- [21] G. L. Raja and A. Ali, “New PI-PD Controller Design Strategy for Industrial Unstable and Integrating Processes with Dead Time and Inverse Response,” *Journal of Control, Automation and Electrical Systems*, vol. 32, pp. 266–280, 2021, doi: 10.1007/s40313-020-00679-5.
- [22] H. I. Ali and A. H. Saeed, “Robust Tuning of PI-PD Controller for Antilock Braking System,” *Al-Nahrain Journal for Engineering Sciences (NJES)*, vol. 20, no. 4, pp. 983–995, 2017. [Online]. Available: <https://www.iasj.net/iasj/download/b9a9585c6e9292fc>
- [23] M. M. Ozyetkin, C. Onat, and N. Tan, “PI-PD controller design for time delay systems via the weighted geometrical center method,” *Asian Journal of Control*, vol. 22, no. 5, pp. 1811–1826, 2020, doi: 10.1002/asjc.2088.
- [24] K. Bingi, R. Ibrahim, M. N. Karsiti, and S. M. Hassan, “Fractional-order PI-PD Control of Real-time Pressure Process,” *Progress in Fractional Differentiation and Applications An International Journal*, vol. 6, no. 4, pp. 289–299, 2020, doi: 10.18576/pfda/060406.
- [25] L. H. Abood and B. K. Oleiwi, “Design of fractional order PID controller for AVR system using whale optimization algorithm,” *Indonesian Journal of Electrical Engineering and Computer Science (IJECS)*, vol. 23, no. 3, pp. 1410–1418, 2021, doi: 10.11591/ijeecs.v23.i3.pp1410-1418.
- [26] V. Mehra, S. Srivastava, and P. Varshney, “Fractional-Order PID Controller Design for Speed Control of DC Motor,” *2010 3rd International Conference on Emerging Trends in Engineering and Technology*, 2010, pp. 422–425, doi: 10.1109/ICETET.2010.123.
- [27] M. M. Ozyetkin, “A simple tuning method of fractional order PI-PD controllers for time delay systems,” *ISA Transactions*, vol. 74, pp. 77–87, 2018, doi: 10.1016/j.isatra.2018.01.021.
- [28] Y. Ahmed, A. Hoballah, E. Hendawi, S. Al Otaibi, S. K. Elsayed, and N. I. Elkalashy, “Fractional order pid controller adaptation for pmsm drive using hybrid grey wolf optimization,” *International Journal of Power Electronics and Drive Systems (IJPEDS)*, vol. 12, no. 2, pp. 745–756, 2021, doi: 10.11591/ijpeds.v12.i2.pp745-756.
- [29] *Digital Pendulum*, Feedback Instrument is Company of LD DIDACTIC Group, 2013. [Online]. Available: [http://www.feedback-instruments.com/pdf/brochures/33-005-PCI\\_datasheet\\_DigitalPendulum\\_MATLAB\\_10\\_2013.pdf](http://www.feedback-instruments.com/pdf/brochures/33-005-PCI_datasheet_DigitalPendulum_MATLAB_10_2013.pdf)
- [30] A. F. Ghaliba and A. A. Oglah, “Design and Implementation of a Fuzzy Logic Controller for Inverted Pendulum System Based on Evolutionary Optimization Algorithms,” *Engineering and Technology Journal*, vol. 38, no. 3A, pp. 361–374, 2020, doi: 10.30684/etj.v38i3a.400.
- [31] S. Gopikrishnan, A. A. Kesarkar, and N. Selvagesan, “Design of fractional controller for cart-pendulum SIMO system,” *2012 IEEE International Conference on Advanced Communication Control and Computing Technologies (ICACCCT)*, 2012, pp. 170–174, doi: 10.1109/ICACCCT.2012.6320764.
- [32] F. Peker and I. Kaya, “Identification and real time control of an inverted pendulum using PI-PD controller,” *2017 21st International Conference on System Theory, Control and Computing (ICSTCC)*, 2017, pp. 771–776, doi: 10.1109/ICSTCC.2017.8107130.
- [33] D. Ibrahim, “An Overview of Soft Computing,” *Procedia Computer Science*, vol. 102, pp. 34–38, 2016, doi: 10.1016/j.procs.2016.09.366.
- [34] S. M. Mahdi, N. Q. Yousif, A. A. Oglah, M. E. Sadiq, A. J. Humaidi, and A. T. Azar, “Adaptive Synergetic Motion Control for Wearable Knee-Assistive System: A Rehabilitation of Disabled Patients,” *Actuators*, vol. 11, no. 7, 2022, doi: 10.3390/act11070176.
- [35] M. A. Hasan, A. A. Oglah, and M. J. Marie, “Packet loss compensation over wireless networked using an optimized FOPI-FOPD controller for nonlinear system,” *Bulletin of Electrical Engineering and Informatics (BEEI)*, vol. 11, no. 6, pp. 3176–3187, 2022, doi: 10.11591/eei.v11i6.4345.
- [36] Q. Tu, X. Chen, and X. Liu, “Hierarchy Strengthened Grey Wolf Optimizer for Numerical Optimization and Feature Selection,” *IEEE Access*, vol. 7, pp. 78012–78028, 2019, doi: 10.1109/ACCESS.2019.2921793.
- [37] S. Mirjalili, S. M. Mirjalili, and A. Lewis, “Grey Wolf Optimizer,” *Advances in Engineering Software*, vol. 69, pp. 46–61, 2014, doi: 10.1016/j.advengsoft.2013.12.007.
- [38] C. Muro, R. Escobedo, L. Spector, and R. P. Coppinger, “Wolf-pack (*Canis lupus*) hunting strategies emerge from simple rules in computational simulations,” *Behavioural Processes*, vol. 88, no. 3, pp. 192–197, 2011, doi: 10.1016/j.beproc.2011.09.006.
- [39] H. Al-Khazraji, “Optimal Design of a Proportional-Derivative State Feedback Controller Based on Meta-Heuristic Optimization for a Quarter Car Suspension System,” *International Information and Engineering Technology Association (IETA)*, vol. 9, no. 2, pp. 437–442, 2022, doi: 10.18280/mmep.090219.
- [40] A. H. Sule, A. S. Mokhtar, J. J. B. Jamian, A. Khidrani, and R. M. Larik, “Optimal tuning of proportional integral controller for fixed-speed wind turbine using grey Wolf optimizer,” *International Journal of Electrical and Computer Engineering (IJECE)*, vol. 10, no. 5, pp. 5251–5261, 2020, doi: 10.11591/IJECE.V10I5.PP5251-5261.
- [41] M. W. Hasan and N. H. Abbas, “An improved swarm intelligence algorithms-based nonlinear fractional order-PID controller for a trajectory tracking of underwater vehicles,” *TELKOMNIKA (Telecommunication, Computing, Electronics and Control)*, vol. 18, no. 6, pp. 3173–3183, 2020, doi: 10.12928/TELKOMNIKA.v18i6.16282.
- [42] J. Huang, T. Zhang, Y. Fan, and J. -Q. Sun, “Control of Rotary Inverted Pendulum Using Model-Free Backstepping Technique,” *IEEE Access*, vol. 7, pp. 96965–96973, 2019, doi: 10.1109/ACCESS.2019.2930220.




**BIOGRAPHIES OF AUTHORS**

**Muhannad A. Hasan**    received a B.Sc. degree in Control and System Engineering from the University of Technology, Baghdad, Iraq in 2004 and 2008 respectively. Currently, he is studying M.Sc. in control and systems engineering department at University of Technology, Iraq. He is interested in wireless network control system study and research. He can be contacted at email: [cse.20.30@grad.uotechnology.edu.iq](mailto:cse.20.30@grad.uotechnology.edu.iq).



**Ahmed A. Oglah**    received his B.Sc. and M.Sc. degrees in Control engineering from Al-Rasheed College of Engineering and Science, University of Technology, Iraq, in 1998 and 2004, respectively. He received his Ph.D. degree from the University of Basrah in 2015 with a specialization in control and computers. He is presently the assistant professor of the computer engineering branch at the Control and Systems Engineering Department at the University of Technology. His interests include intelligent control systems, nonlinear control systems, robotics, computer networks, image processing, digital systems design, real-time systems and optimization techniques. He can be contacted at email: [Ahmed.A.Oglah@uotechnology.edu.iq](mailto:Ahmed.A.Oglah@uotechnology.edu.iq).



**Mehdi J. Marie**    was born in Baghdad, Iraq in 1970. He received his Bachelor's (1993), Master's (2004) Degrees from University of Technology (Iraq) and Ph. D. from the University of Basrah (2014). He has been a lecturer of Control Theory I, II, Electrical Networks, Advanced Electronics and Soft Computing Techniques (2014-2017) at the Al-Nahrain University, Computer Engineering Department. He is currently a Senior Engineer at Al-Zawraa State Company, Ministry of Industry and Minerals (Iraq). He has achieved over 11 Journal articles and 9 conference papers in the field of Control Engineering and Systems. He can be contacted at email: [mehdijelo@gmail.com](mailto:mehdijelo@gmail.com).